# Identification of Laser-induced Lamb waves

M. Castro-Colin
*Physics Department, U.T. El Paso, El Paso, TX 79968.*

J.A. Lopez
*Physics Department, U.T. El Paso, El Paso, TX 79968.*

R. Osegueda
*FAST Center, Burgess Hall, U.T. El Paso, El Paso, TX 79968.*

Recibido el 2 de marzo de 2006; aceptado el 18 de agosto de 2006

We studied experimentally the ultrasonic propagating modes produced by a laser pulse of 532 nm while impinging on an aluminum plate. The beam, shaped as a line, induced various Lamb modes whose relative power varied with the laser line length. Identification of their mode was performed by detecting the ultrasonic modes with piezoelectric detectors along a propagation direction orthogonal to the line, and using two dimensional fast Fourier transform. Good agreement is observed between theoretical and experimental dispersion curves for the first fundamental symmetric and anti-symmetric modes. Results are shown for 12 and 24 mm laser line-length at 13.6 and 16.8 ns pulse-width.

*Keywords:* Laser based ultrasound; non-destructive testing; photoacoustic.

Se presenta el estudio experimental de los modos ultrasónicos de propagación producidos por el impacto de un pulso laser de 532 nm en una placa de aluminio. El haz, con forma de una línea, induce varios modos de Lamb cuya potencia relativa varía con la longitud de la línea del láser. La identificación del modo correspondiente se realizó detectando los modos ultrasónicos con detectores piezoeléctricos a lo largo de la dirección ortogonal a la propagación de la línea y utilizando una transformada de Fourier en dos dimensiones. Buen acuerdo se obtiene entre las predicciones teóricas y las curvas de dispersión medidas experimentalmente para los primeros modos fundamentales simétrico y antisimétrico. Los resultados se muestran para longitudes de línea de 12 y 24 mm a 13.6 y 16.8 ns de anchura de pulso.

*Descriptores:* Ultrasonido originado con láser; pruebas no destructivas; fotoacústica.

PACS: 42.62.Cf; 81.70.Cv; 43.35.Zc; 43.35.Ud

## 1. Introduction

Conventional ultrasonic techniques employing piezoelectric transducers (PZTs) are well established for flaw detection, and have made a major contribution to quality assurance and structural integrity. Laser-induced ultrasound aims at selectively producing vibrational modes with applications in non-destructive evaluation purposes. In particular for sheets, ultrasound waves refer to Lamb waves which are vibrations generated in media with two free surfaces [1, 2]. YAG and ruby lasers have been used combined with Fresnel arrays [3] and lenses [4] to induce single mode Lamb waves. Since mode conversion is the main problem faced while Lamb waves interact with defects [5], in this work we investigated ways of selectively inducing single mode waves [3, 4, 6–8]. We used a 532 nm laserlight from a Q-switched Nd:YAG to investigate the effect that pulse-width and beam geometry have on Lamb waves induced on thin (1 mm) aluminum plates. In particular we focus the possibility of wave mode selection through variation of pulse-width and laser line length. The laser power has been kept well below the ablation regime [7] to ensure only thermoelastic ultrasonic generation that avoids damage to the aluminum.

## 2. Theoretical background

In order to identify the modes excited in the aluminum plates of interest here, we solve the transcendental Rayleigh-Lamb equation [2, 9] numerically:

$$\frac{\tan k_d b}{\tan k_t b} = -\left[\frac{[{k_0}^2 - {k_t}^2]^2}{4{k_0}^2 k_d k_t}\right]^{\pm 1} \tag{1}$$

In Eq. (1) + and - refer to symmetric and antisymmetric waves, respectively, while $k_d$ represents the longitudinal propagation mode and $k_t$ represents the transverse mode (${k_d}^2 = \omega^2/{c_d}^2 - {k_0}^2$ and ${k_t}^2 = \omega^2/{c_t}^2 - {k_0}^2$; $k_0 = \omega/v$; $v$ = phase velocity). $c_d$ and $c_t$ directly involve the physical parameters of the material [2, 9]:

$${c_d}^2 = \frac{\lambda + 2\mu}{\rho}, \qquad {c_t}^2 = \frac{\mu}{\rho} \tag{2}$$

and

$$\lambda = \frac{\sigma E}{(1+\sigma)(1-2\sigma)}, \qquad \mu = \frac{E}{2(1+\sigma)} \tag{3}$$

The physical properties of aluminum used in solving Eq. (1), were: $\rho$ = 2.70 g·cm$^3$ (density), $\sigma$ = 0.345 (Poisson's ratio) and $E$ = 70.6 GPa (Young's modulus).

## 3. Experimental setup

The instrumentation used in this experimental investigation is shown schematically in Fig. 1. A series of pulses from a Nd:YAG laser laser were used to excite elastic waves in an aluminum plate. The laser beam was optically distorted into a line shape of controllable length. The ultrasound waves produced were detected by means of PZTs (Digital Wave B1025)

placed on the plate. The PZT signal was then amplified and collected for further analysis.

The Nd:YAG laser available for this study is able to emit at 1064, 532, 355, and 266 nm wavelengths. The fundamental wavelength is located within the IR spectrum, while the third and fourth harmonics fit in the UV. Although, due to absorption properties, it would be desirable to use either UV wavelength [10], the second harmonic is the only visible wavelength and at this stage visible light eases control of the experimental parameters, thus the fundamental wavelength, 532 nm, was used to substantially ease the beam alignment. During our experiments the laser power density is kept below the ablation power density [7], avoiding any visible damage to the plate. With an incident angle of 5 degrees between the laser and the material surface, the interaction was then purely thermoelastic. The laser has a synchronization signal that occurs 170 ns before the output. This fixed synchronization output is thus used to establish a time reference for all events, as well as to trigger signal capture in the oscilloscope. As a second check on laser firing, we also used a ultra-fast photodiode, MRD510, with a threshold response well within the wavelenth in use. To distort the circular beam into a line-shaped beam, an optical arrangement consisting of an optical density filter, a plane-concave lens, a plane-convex lens, a cylindrical lens, and a high energy laser mirror were used. Plane-concave and plane-convex lenses, with effective focal lengths of 30 and 50 mm respectively, condense the laser beam from 6 mm down to 1 mm diameter. The cylindrical lens, 44 mm focal length, stretches the circular beam into a line, maintaining a 1 mm width dimension while allowing a line-length variation through altering the incident angle appropriately.

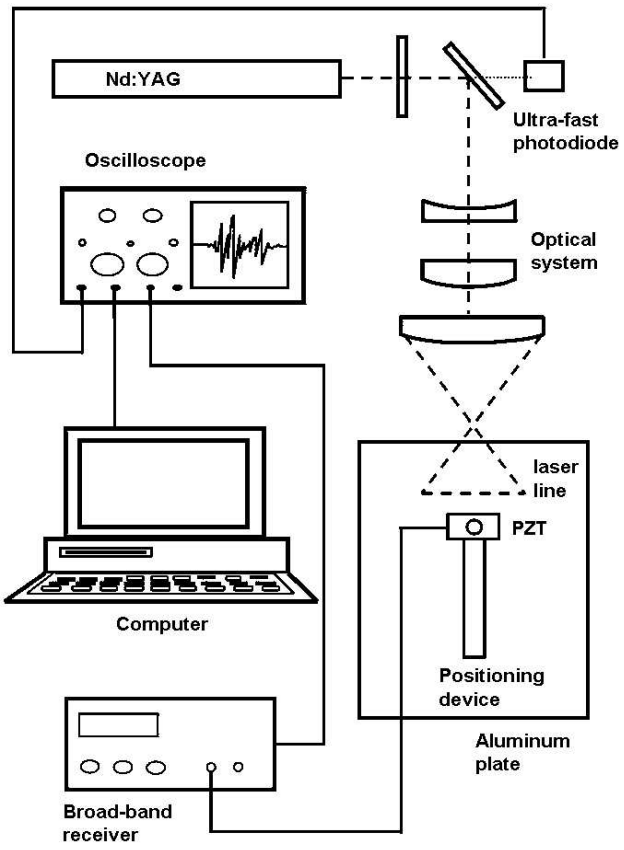


FIGURE 1. Schematic of the experimental setup for laser-based ultrasonic system.

For the ultrasound wave detection, PZTs with a collection bandwidth of 1 kHz to 1.5 MHz were used. The signal captured from the PZT is then amplified by a broadband receiver (Matec 605) with a 100 kHz - 25 MHz bandwidth, and sent to an oscilloscope (Tektronix TDS420A) for display. LabView was used to capture the signal data, as well as to control the laser trigger. The computer code permits interfacing the oscilloscope to the computer through a GPIB board.

As with any other resonant system, an aluminum plate can vibrate with a number of modes which move at different velocities. Energy deposited by laser light, in this case, can induce several resonant modes. Their sucessful ideantification consists of characterizing both frequency and wave-number information. This cannot be done with a simple harmonic analysis of the time signal collected by the PZT, thus an alternative technique is used to identify these resonant modes. Mode identification can be accomplished via time-frequency analysis [11]. Using time signals obtained at different spatial locations and analyzed via the following two-dimensional Fourier transform [12, 13]:

$$U_{k,f} = \frac{1}{N \times M} \sum_{x=1}^{M} \sum_{t=1}^{N} u_{x,t} e^{-i\left(\frac{k}{M} + \frac{2\pi f}{N}\right)} \qquad (4)$$

Equation 4 helps in identifying points on the dispersion curves directly. Time records obtained at different locations are transformed into wave-number records at discrete frequencies. Superposition of the 2D-FFT data to the solutions of Rayleigh-Lamb equations [2, 9] (*i.e.* against the response function of the aluminum plate) allowed us to obtain group velocity, $c_g = \delta\omega/\delta k$ [11], information. To implement this technique experimentally, the PZT is placed at different spatial locations where it captures a signal. 32 to 64 equally spaced intervals are selected along a line orthogonally directed away from the point of impact of the laser beam. At each position a 2500 time-length record was stored. All measurements were combined into a $32\times2048$ (or $64\times2048$) matrix (N, M). The Fast Fourier transform is applied along the spatial and time directions. Frequency and wave number are this way identified. The parameters used were $\Delta x$ = 0.508 mm and $\Delta t$ = 100 ns.

## 4. Results

Experiments were performed for laser line lengths of 12, 24, 36, 47 and 56 mm, and pulse-widths 16.8, 14.0, 13.6 and 13.4 ns (the average power was 7, 17, 19, and 22 mW, respectively). A total of 20 effective experiments were performed,

of which only the most significative results are shown below. Characteristic results of our experiment and analysis are shown in Figs. 2 and 3. Figure 3 shows the dispersion plane with the main modes detected in the aluminum plate when using a 13.6 ns and 24 mm laser line-length. In this case the relative amplitudes of modes along the symmetric branch, $s_0$, of the dispersion curve reach half the amplitude of the main antisymmetric $a_0$ mode. Likewise Fig. 4 shows the corresponding results for 14.0 ns pulse-width and 24 mm laser line-length. In this last case the $a_0$ mode is predominant. The relative amplitudes can be better observed in Figs. 3 and 4. Due to the reduction in pulse-width, Fig. 3 exhibits a signal with more structure than Fig. 5, although the same laser line-length, 24 mm, was used; the relative amplitude of the $s_0$ mode is about 1/3 of the $a_0$ mode. It is thus clear that pulse-width and beam-length can be chosen so as to selectively modify the spectral content of the induced Lamb waves.

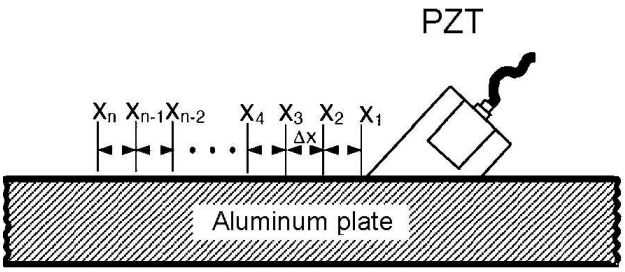


FIGURE 2. Schematic of data collection technique. The piezoelectric transducer (PZT) is coupled to a perspex wedge that makes contact with the aluminum plate through a couplant gel.

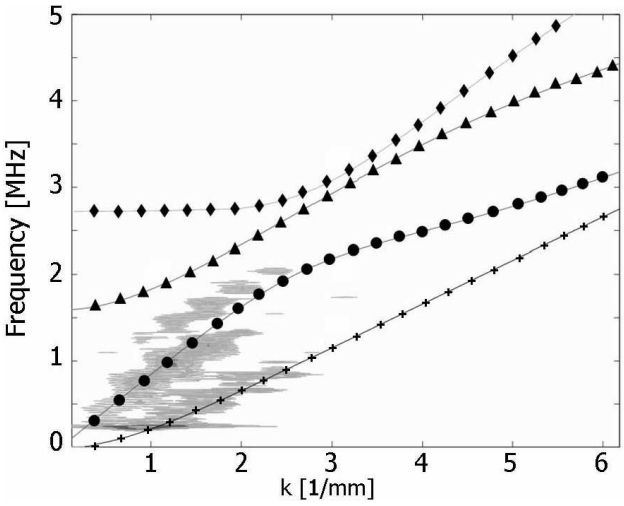


FIGURE 3. 2D-FFT experimental data superimposed on numerically calculated dispersion curves, 13.6 ns pulse-width and 24 mm laser line-length (contour plot). The aluminum plate has a thickness of 1.58 mm. The dispersion curves represented are: $a_0$ (cross), $s_0$ (full circle), $a_1$ (full triangle), $s_1$ (full diamond).

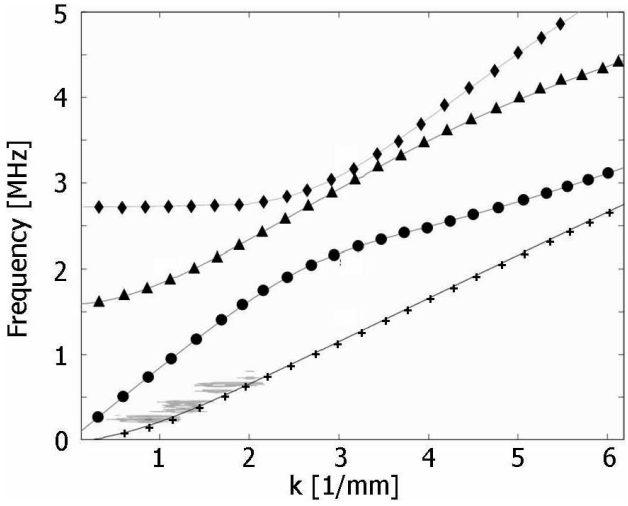


FIGURE 4. 2D-FFT experimental data superimposed on numerically calculated Lamb wave dispersion curves, 14.0 ns pulse-width and 24 mm laser line-length (contour plot). The aluminum plate has a thickness of 1.58 mm. The dispersion curves represented are: $a_0$ (cross), $s_0$ (full circle), $a_1$ (full triangle), $s_1$ (full diamond).

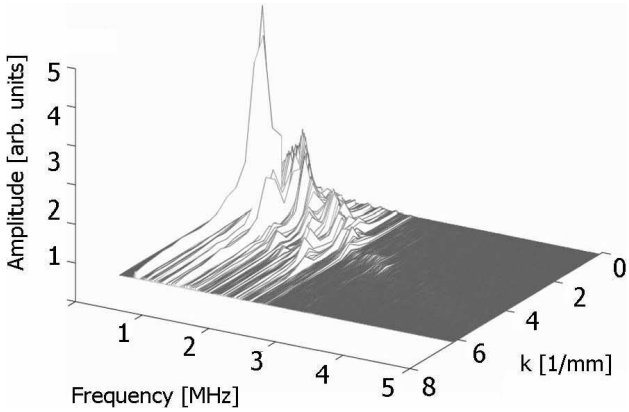


FIGURE 5. 3D-plot of 2D-FFT experimental data, 13.6 ns pulse-width and 24 mm laser line-length (1.58 mm aluminum plate thickness).

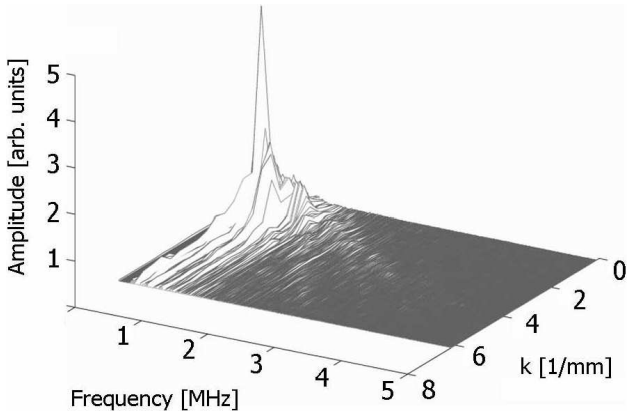


FIGURE 6. 3D-plot of 2D-FFT experimental data, 14.0 ns pulse-width and 24mm laser line-length (1.58 mm aluminum plate thickness).

## 5. Conclusions

Ultrasonic techniques are well established for flaw detection. To reduce the problem of mode mixture and conversion, laser-induced ultrasonic methods attempt to produce single Lamb wave modes in sheets. In this work we investigated the effect of pulse-width and beam geometry as parameters that induce mono-modal Lamb waves. Using a 532 nm laser pulse, optically distorted into a line shape, elastic waves were produced in an aluminum plate. The 2D-FFT showed to be a valuable tool in identifying the vibrational modes. Modes $s_0$ and $a_0$ constituted the main spectral content of Lamb modes present. In particular, our results show that a 14.0 ns pulse-width and a 24 mm laser line-length are the most suitable parameters for non-destructive flaw-detection purposes, since such combination of pulse-width and laser source, yielded an enhanced 250 kHz and 1 mm$^{-1}$, $a_0$ mode (see Fig. 6), which simplifies the spectral input that can later be used in structural integrity of aluminum sheets.

## Acknowledgements

This work was partially supported by the National Science Foundation under grant PHYS-1996, and FAST under grant number F4962-95-1-0518, Air Force Office of Scientific Research, Air Force Materiel Command, USAF. We acknowledge constructive discussions with E. Rodriguez and S. Nazarian.

1. W.J. Percival and E.A. Birt, *J. Acoust. Soc. Am.* **100** (1996) 3070.
2. I. A. Viktorov, *Rayleigh and Lamb waves* (Ed. Plenum Press, New York 1967).
3. R.D. Costley Jr. and Y.H. Berthelot, *Ultrasonics* **32** (1984) 249.
4. R.C. Addison and A.D.W. MacKie, *1994 Ultrasonics Symposium IEEE* (1994) 1201.
5. D.N. Alleyne and P. Cawley, *IEEE Transactions on Ultrasonics, Ferroelectrics, and FrequencyControl* **39** (1992) 381.
6. R.D. Costley Jr., Y.H. Berthelot, and L.J. Jacobs, *J. Nondestr. Test.* **13** (1994) 33.
7. B. Mi and I.C. Ume, *J. Nondestr. Test.* **21** (2002) 23.
8. M.D.G. Potter and S. Dixon, *Nondestr. Test. and Eval.* **20** (2005) 201.
9. E. Dieulesaint and D. Roger, *Elastic waves in solids: applications to signal processing* (Ed. John Wiley and Sons, New York 1980).
10. C.B. Scruby *et al. Laser ultrasonics: techniques and applications* (Ed. Adam Hilger, Bristol, Philadelphia and New York 1990).
11. W. Sachse and Y-H Pao, *J. Appl. Phys.* **49** (1978) 4320.
12. J.W. Cooley and J.W. Tukey, *Math. Comput.* **19** (1965) 297.
13. H. Guo, G.A. Sitton, and C.S. Burrus, *Proc. IEEE Conf. Acoust. Speech and Sig. Processing (ICASSP)* **3** (1994) 445.